


Research Article

Effect of Curing Temperature and Time on Mechanical Properties of Vinyl Polymer Material for Sealing Applications in Industry Using Machine Learning Techniques

Sudheer D. Kulkarni ^{1,2}, B. Manjunatha,³ U. Chandrasekhar,⁴ G. K. Siddesh ⁵,
Haider Lenin ⁶ and Sujin Jose Arul⁷

¹New Horizon College of Engineering, Visvesvaraya Technological University, Bangalore, India

²Department of Industrial Engineering and Management, Ramaiah Institute of Technology, Bangalore 560054, India

³Professor, Department of Mechanical Engg, New Horizon College of Engineering, Bengaluru, Karnataka, India

⁴AddWize-Wipro 3D, Bangalore 560058, India

⁵ECE Department and Deputy Dean Research, ALVA'S Institute of Engineering and Technology, Moodbidri, DK, Karnataka, India

⁶Department of Mechanical Engineering, WOLLO University, Kombolcha Institute of Technology, Kombolcha, Ethiopia Post Box No: 208

⁷Department of Automobile Engineering, New Horizon College of Engineering, Bangalore, India

Correspondence should be addressed to Haider Lenin; haider@kiot.edu.et

Received 24 January 2023; Revised 11 March 2023; Accepted 29 April 2023; Published 16 May 2023

Academic Editor: Indran Suyambulingam

Copyright © 2023 Sudheer D. Kulkarni et al. This is an open access article distributed under the Creative Commons Attribution License, which permits unrestricted use, distribution, and reproduction in any medium, provided the original work is properly cited.

A seal is a mechanism or a piece of material that securely shuts a hole so that air, liquid, or other substances cannot enter or exit the system. Seals are an essential component of practically all machinery and engines and have several applications in industry. The development of novel materials for sealing applications is essentially required on these days. In this research, an attempt is made to find the polymer material for the said application. Poly vinyl rubber material has been taken, and the specimens are prepared for testing the tensile properties and hardness. The specimens were prepared by using die with various temperatures and curing time. Sixteen specimens were prepared by changing the curing temperature, curing time, postcuring temperature, and postcuring time. The curing temperature 150°C and 170°C, postcuring temperature 100°C and 50°C, curing time 14 mins and 18 mins, postcuring time 120 mins and 60 mins, and the pressure of 150 kg/cm² for all the specimens were maintained. The tensile strength and hardness analysis were done as per the ASTM standard, and it was found that the specimen prepared on 150°C curing temperature, 18 min curing time, 50°C postcuring temperature, and 120 min postcuring time provides the higher tensile strength. DOE analysis is also done to determine the best values of the factors impacting the mechanical characteristics of the seal material. Simple regression analysis is used to find the influence of curing temperature and curing time on the tensile strength and hardness for every 1°C temperature rise and 1 sec curing time.

1. Introduction

A versatile and cost-effective material, “polyvinyl chloride (PVC, or vinyl) is used in plumbing and siding, blood bags, tubing, wire and cable insulation, windshield system components, and more, in the building and construction, health care, electronics, automobile industries, and others.” Vinyl can range in hardness from plastic wrap to industrial pipes

to thin and flexible wall covering. Additionally, it can be completely translucent or colored to any desired shade. The majority of vinyl produced is employed in long-term building and construction applications—roughly 75%. PVC/vinyl is advantageous for environmental protection because of its low greenhouse gas emissions and ability to conserve resources and energy, according to life-cycle studies. Since vinyl is strong and resistant to moisture and

abrasion, it is ideal for cladding, windows, roofs, fences, decks, wall coverings, and flooring. Contrary to some building materials, vinyl is not prone to corrosion, does not need to be painted frequently, and can be cleansed using straightforward cleaning solutions. VTI employs RF welding, also known as dielectric welding. This is a procedure that uses radio frequency waves to molecularly fuse two films or textiles together, forming a hermetic connection [1]. This is a procedure with several names, and you may have heard one of them: dielectric sealing, RF sealing, RF welding, and heat sealing [2]. They all refer to the same high-tech approach of connecting thermoplastic sheets that use radio frequency (RF) radiation. RF waves excite the molecules of the materials, causing them to fuse together from the inside out [3, 4]. Depending on your use, it does not leak air, moisture, water, or fuel. High frequency radio waves are used to heat the material in RF sealing, which is similar to heat sealing [5]. Radio waves (typically between 15 kHz and 70 kHz) cause polymer molecules to vibrate, which generates a significant amount of heat quickly. In this way, RF seals are faster, more consistent, and stronger than conventional heat seals. Because exposed seals are transparent and flawless, this procedure is also suitable for them [6]. It is more expensive and requires more energy to perform RF sealing than a traditional heat seal; nevertheless, the field of RF sealing is rapidly evolving and becoming more efficient [7]. The use of RF sealing to polyvinyl chloride or vinyl fabric is known as PVC sealing. Because of its flexibility and polarity, PVC is an excellent choice for RF heat sealing. It is also ideal for generating hermetic seals and waterproofing applications. PVC sealing is a high-frequency welding procedure that allows PVC (polyvinyl chloride) to be applied to a soft fabric or film [8, 9]. PVC is used in waterproofing textiles because it is lightweight, resilient, and abrasion resistant. Because of its high dipolar moment and other chemical features, PVC is regarded as a suitable material for radio frequency welding [10, 11]. PVC welding is a comparable procedure in which PVC is used as the material of choice when welding textiles, plastics, or other materials together. Another name for RF sealing is HF welding, which is used interchangeably [12, 13]. Both words refer to the method of joining two thermoplastic polymers using high-frequency radio waves. This procedure is also known as RF heating, HF heating, and dielectric sealing.

PVC sheets and boards, in particular, can benefit from the strong seams produced by RF welding [14, 15]. The products of the PVC sealing technique can be flexible and elastic while yet having shear strength and durability [16]. PVC is a versatile and cost-effective material in and of itself. Its primary advantages are as follows:

Electrical insulation: because PVC has a high dielectric strength, it is an excellent insulation material for electrical purposes. Abrasion, weathering, oily residues, greases, chemical degradation, corrosion, and pressure all resist PVC [17, 18]. Since durability is a primary requirement for many outdoor products, it makes sense that it is the material of choice. Because of their high chlorine content, PVC goods are self-extinguishing [19]. This offers a great fire resistance and mechanical qualities.

High performance at a low cost: the durability and other features listed above enable for completed goods that require little maintenance and replacement in a variety of environmental circumstances [20]. Because PVC is abrasion-resistant, lightweight, and durable, it is the material of choice for completed items that will be subjected to weathering or hard use.

Poly vinyl seal material is being evaluated experimentally for its mechanical characteristics in relation to process factors. The particular aims, technique to be used to achieve the objectives, and possible outcomes are detailed in the following sections. Dong et al. [21] examined the effect of poly vinyl alcohol/aluminum microcapsule expansion agents on cement-based drilling sealing materials, and the effect of delayed expansion on mechanical strength, porosity, and pore connectivity of the sealing material is quantitatively examined using uniaxial compression and NMR experiments. Ethylene-propylene diene monomer rubber was proposed as a viable option for recycling end-of-life poly vinyl chloride foams by Mahmood et al. [22]. The effects of high-pressure processing on the properties of multilayer flexible packaging are made of polyamide and ethylene vinyl alcohol. The findings of this study have implications for the food packaging industry, particularly in terms of developing packaging materials that can withstand high-pressure processing while maintaining their mechanical and thermal properties [23]. A variety of volumes of ethylene-propylene diene monomer (EPDM) rubber and carbon black (CB) were combined with EoL PVC cross-linked foams at 60°C for 15 minutes. Compression moulding of EPDM-CB-PVC composites was achieved by vulcanizing the rubber mixtures for 20 minutes at 160°C. In tensile tests, EPDM-CB's modulus gradually increased with increasing PVC content, while its elongation-at-break decreased. In the EPDM-CB matrix, PVC particles were dispersed uniformly by SEM. A multidisciplinary approach to biomedical applications using poly vinyl pylori done electro spun nanofibers and bioprinted scaffolds was established by Kurakula et al. and Kibirikšis et al. [24, 25]. The tensile strength of polymer specimens with varying infill density is better than the specimens with single infill density [26–30]. Through the study, it is concluded that the vinyl polymer will be the best alternative for sealing material.

2. Materials and Methods

2.1. Materials. Poly vinyl rubber has been taken as a material for making seal and underwent the mechanical property analysis. The test specimens were prepared in M/s Seal Industries Pvt. Ltd., Bangalore, Karnataka State, India, for conducting the experiment trials. The procured material has the density of 1.05 gm/cm³.

2.2. Specimen Preparation. The specimens were prepared using die for testing that was shown in Figure 1. The die was preheated to a temperature of 150°C, and the poly vinyl rubber compound was placed on the cavity of die. The die closed, and the pressure of 150 kg/cm² was applied on the die, and it was allowed for 14 minutes of curing. In the same

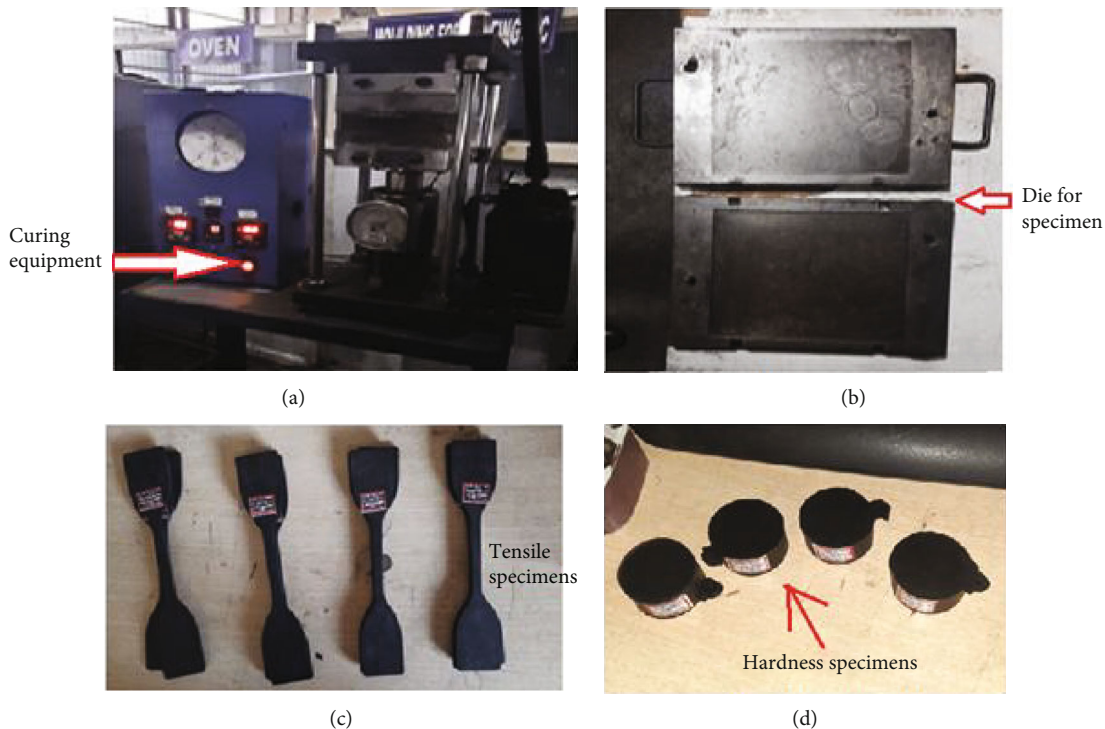


FIGURE 1: (a) Curing equipment. (b) Die set. (c) Tensile specimens. (d) Hardness specimens.

TABLE 1: Process control parameters and specimens.

| Specimen number | Curing temp. in °C | Curing time in mins | Postcuring temp. in °C | Postcuring time in mins |
|-----------------|--------------------|---------------------|------------------------|-------------------------|
| 1 | 150 | 14 | 100 | 60 |
| 2 | 150 | 14 | 100 | 120 |
| 3 | 150 | 14 | 50 | 60 |
| 4 | 150 | 14 | 50 | 120 |
| 5 | 150 | 18 | 100 | 60 |
| 6 | 150 | 18 | 100 | 120 |
| 7 | 150 | 18 | 50 | 60 |
| 8 | 150 | 18 | 50 | 120 |
| 9 | 170 | 14 | 100 | 60 |
| 10 | 170 | 14 | 100 | 120 |
| 11 | 170 | 14 | 50 | 60 |
| 12 | 170 | 14 | 50 | 120 |
| 13 | 170 | 18 | 100 | 120 |
| 14 | 170 | 18 | 100 | 60 |
| 15 | 170 | 18 | 50 | 60 |
| 16 | 170 | 18 | 50 | 120 |

way, another specimens were prepared by changing the die preheating temperature as well as curing time. After curing time, the pressure was released, and the die opened. The desired rubber sheet was taken out from the die and allowed to aging for 24 hours at a room temperature. After aging, the tensile and hardness specimens were cut from the sheet as per the ASTM dimensions.

2.3. *Tensile Test.* Tensile tests were performed using a universal testing machine to measure tensile strength, load at break, and % elongation at various combinations. ASTM D903 was used as the testing standard. With a grip gap of 25 mm, the specimen is mounted between the grips. The system’s readings are reset to zero. A load is applied gradually until the specimen fails.

3. Results and Discussions

The tensile strength of various specimens tested and taken 3 trials as per the ASTM standard, and the optimization was done on the results.

3.1. *Design of Experiment Analysis.* For this investigation, the response variables were tensile strength, modulus at 100%, and percentage elongation. The experiment used 24 designs with three repetitions to determine the best values of the factors impacting the mechanical characteristics of the seal material. The run order for these tests was generated using Minitab software. Table 1 shows the factors examined and their range values. Table 2 represents the performance analysis. The experiment was conducted using the DOE approach, with two levels and four components, for a total of 24 complete factorial designs. Pilot runs were carried out to check that the equipment worked properly. The procedure was meticulously watched to ensure that everything went as planned. According to the experimental design, the settings were chosen. In order to account for the operational peculiarities, standard order was created. To avoid the influence of noise, the experiment was conducted in a random sequence. The experiments were all random. Standard and

TABLE 2: Average tensile strength and hardness values of specimens.

| Specimen number | Extension (mm) | Displacement (mm) | Peak load (N) | Yield load (N) | Tensile strength N/mm ² | Hardness (HB) |
|-----------------|----------------|-------------------|---------------|----------------|------------------------------------|---------------|
| 1 | 42.60 | 102.50 | 86.595 | 86.595 | 7.2167 | 69 |
| 2 | 41.90 | 113.90 | 85.222 | 85.222 | 7.1001 | 71 |
| 3 | 49.80 | 121.50 | 85.22 | 85.22 | 7.1001 | 67 |
| 4 | 43.70 | 102.50 | 75.61 | 75.61 | 6.3008 | 68 |
| 5 | 43.00 | 107.50 | 89.635 | 89.635 | 7.4687 | 70 |
| 6 | 42.90 | 102.50 | 94.049 | 94.049 | 7.8375 | 69 |
| 7 | 48.10 | 122.50 | 94.54 | 94.54 | 7.8777 | 69 |
| 8 | 53.10 | 129.10 | 99.34 | 99.34 | 8.2778 | 70 |
| 9 | 48.20 | 122.70 | 94.931 | 94.931 | 7.911 | 71 |
| 10 | 42.90 | 102.50 | 91.891 | 91.891 | 7.657 | 71 |
| 11 | 51.10 | 126.10 | 95.422 | 95.422 | 7.9512 | 69 |
| 12 | 47.80 | 122.70 | 94.931 | 94.931 | 7.91102 | 68 |
| 13 | 47.70 | 124.00 | 98.462 | 98.462 | 8.2042 | 69 |
| 14 | 54.50 | 134.10 | 95.814 | 95.814 | 7.9836 | 68 |
| 15 | 52.70 | 128.20 | 87.95 | 87.95 | 7.3292 | 68 |
| 16 | 50.00 | 124.00 | 94.049 | 94.049 | 7.8375 | 69 |

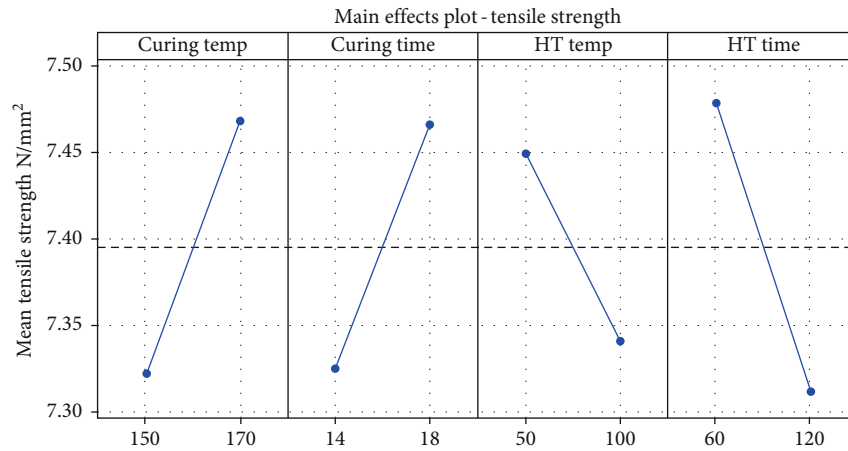


FIGURE 2: Effects of tensile strength.

run orders must be specified. Minitab software was used to create plots of main effects and interaction effects. Figure 2 illustrates the effects of tensile strength, and Figure 3 is its interaction plot.

Figure 4 displays the specimens' weight vs. infill density, break load, and peak load. The break value and peak load of specimen C were found to be the lowest, measuring "686.5 N and 725.7 N," respectively. Among the single infill density specimens A, B, and C, specimen A had the highest value, which was determined to be "1088.6 N and 1127.8 N," respectively. The experimental data clearly show that load-bearing capacity rises with a positive incremental change in infill density. The highest break and peak load among the specimens of combined infill density are determined to be "1000.3 N and 1122.9 N" in specimen ABA from the results. The least break and peak load values for the specimen CBC are "779.7 N and 872.85 N," respectively. The experimental data set aids in understanding how the specimen fails and

how the crack spreads from the outside layer to the inside layer. In the following section, this event is explained in more detail. One of the significant elements affecting the tensile property is the variation in the density of the filling layers in their layering order.

3.2. Correlation Analysis on Factors Affecting Tensile Strength. Correlation analysis has been done using the Pearson correlation coefficient (Equation (1)) to understand the correlation between the independent variables and dependent variable. Curing times and curing temperatures are the independent variables which are affecting the tensile strength. Tensile strength is the dependent variable which varying based on the variable curing temperature and curing time.

$$r = \frac{n\sum xy - (\sum x)(\sum y)}{\sqrt{[n\sum x^2 - (\sum x)^2][n\sum y^2 - (\sum y)^2]}} \quad (1)$$

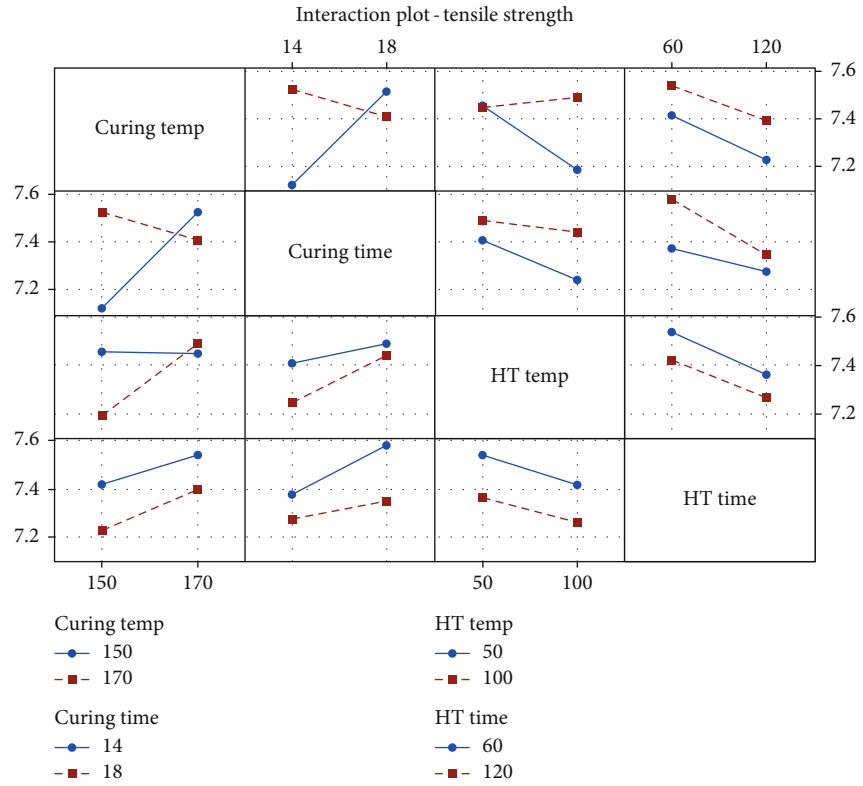


FIGURE 3: Interaction plot for tensile strength.

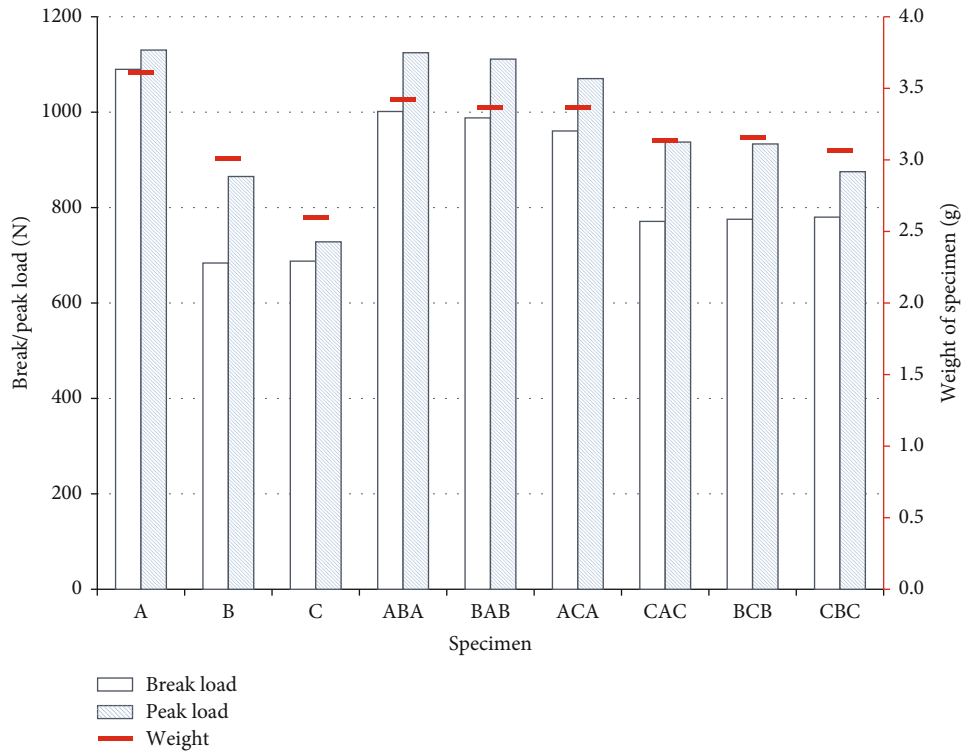


FIGURE 4: Peak load and break load during a tensile test are compared.

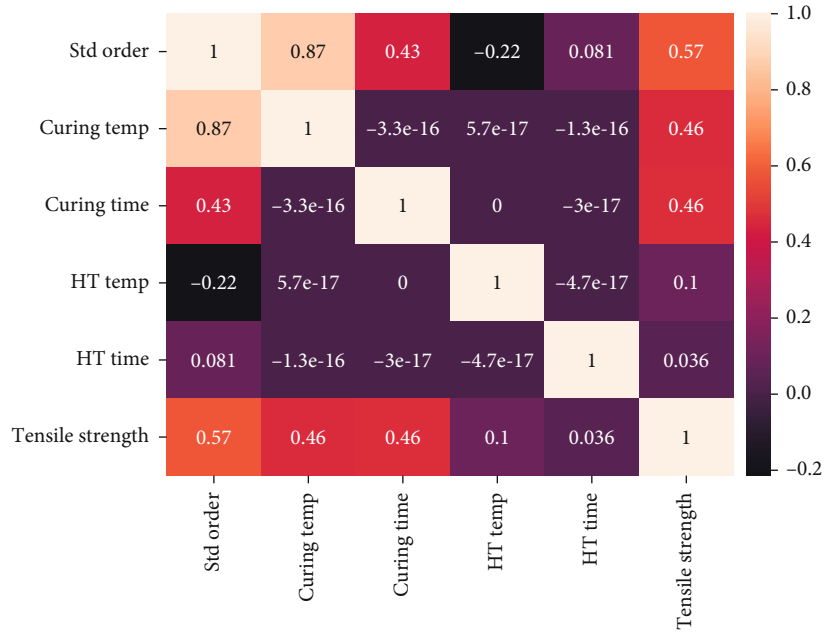


FIGURE 5: Correlation map.

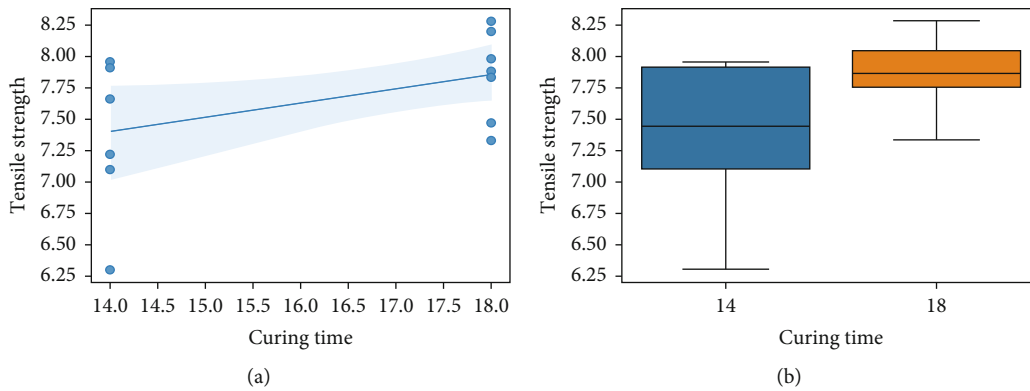


FIGURE 6: Tensile strength vs. curing time: (a) scatter plot and (b) box plot.

Results: Ordinary least squares

| | | | |
|---------------------|------------------|---------------------|---------|
| Model: | OLS | Adj. R-squared: | 0.182 |
| Dependent variable: | Tensile strength | AIC: | 19.3050 |
| Date: | 2023-02-22 11:56 | BIC: | 20.2748 |
| No. observations: | 12 | Log-likelihood: | -7.6525 |
| Df model: | 1 | F-statistic: | 3.448 |
| Df residuals: | 10 | Prob (F-statistic): | 0.0930 |
| R-squared: | 0.256 | Scale: | 0.25154 |

| | Coef. | Std. err. | t | P > t | [0.025 | 0.975] |
|-------------|--------|-----------|--------|--------|---------|--------|
| Const | 5.3794 | 1.2079 | 4.4536 | 0.0012 | 2.6881 | 8.0707 |
| Curing time | 0.1363 | 0.0734 | 1.8568 | 0.0930 | -0.0273 | 0.2999 |

| | | | |
|-----------------|--------|-------------------|-------|
| Omnibus: | 0.843 | Durbin-Watson: | 1.854 |
| Prob (Omnibus): | 0.656 | Jarque-Bera (JB): | 0.476 |
| Skew: | -0.454 | Prob (JB): | 0.788 |
| Kurtosis: | 2.641 | Condition no.: | 138 |

FIGURE 7: Linear model summary for tensile strength vs. curing time.

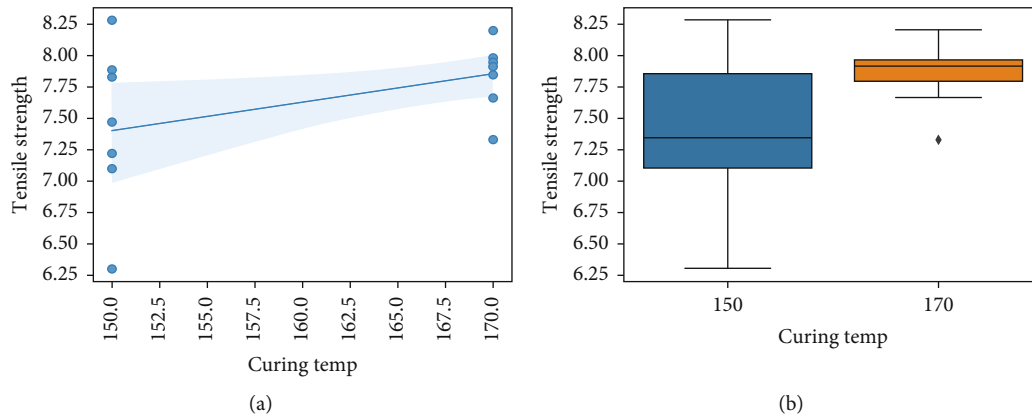


FIGURE 8: Tensile strength vs. curing temperature: (a) scatter plot and (b) box plot.

| Results: Ordinary least squares | | | | | | |
|---------------------------------|------------------|---------------------|---------|--------|---------|---------|
| Model: | OLS | Adj. R-squared: | 0.051 | | | |
| Dependent variable: | Tensile strength | AIC: | 21.0911 | | | |
| Date: | 2023-02-22 12:06 | BIC: | 22.0609 | | | |
| No. observations: | 12 | Log-likelihood: | -8.5455 | | | |
| Df model: | 1 | F-statistic: | 1.588 | | | |
| Df residuals: | 10 | Prob (F-statistic): | 0.236 | | | |
| R-squared: | 0.137 | Scale: | 0.29191 | | | |
| | Coef. | Std. err. | t | P > t | [0.025 | 0.975] |
| Const | 4.4498 | 2.5094 | 1.7733 | 0.1066 | -1.1415 | 10.0410 |
| Curing temp | 0.0199 | 0.0158 | 1.2602 | 0.2362 | -0.0153 | 0.0552 |
| Omnibus: | 2.430 | Durbin-Watson: | 2.869 | | | |
| Prob (Omnibus): | 0.297 | Jarque-Bera (JB): | 0.783 | | | |
| Skew: | -0.608 | Prob (JB): | 0.676 | | | |
| Kurtosis: | 3.294 | Condition no.: | 2552 | | | |

FIGURE 9: Linear model summary for tensile strength vs. curing temperature.

The correlation between the independent variables and dependent variable is shown in Figure 5. This statistical measure indicates how far the variables changes according to each other. As shown in Figure 5, there is a positive correlation between the independent variables such as curing time and temperatures and the expected tensile strength.

3.3. Effect of Curing Time on Tensile Strength. The tensile strength is influenced by curing time which is shown in Figure 6. Figure 6(a) reveals the correlation between the curing time and tensile strength. The variation of tensile strength is calculated by Equation (2). Figure 6(b) represents the numerical data used to understand the variability of the data and the presence of out layers which describes the statistics of various quartiles, the maximum and minimum values of tensile strength and interquartile range.

$$y = \alpha + \beta x. \tag{2}$$

The linear model summary is used to diagnose the regression model which is shown in Figure 7.

The independent parameter is chosen to be curing time (x), and the linear model is given as

$$\text{Tensile strength} = 5.379 + 0.136 \times \text{curing time}. \tag{3}$$

From the analysis, it is clear that, for every 1 sec increase of curing time, the tensile strength will increase by 0.136 N/mm².

3.4. Effect of Curing Temperature on Tensile Strength. Curing temperature and postcuring temperature are also making the influence on tensile strength of the specimen. The scatter plot (Figure 8(a)) reveals the correlation between the curing temperature and tensile strength. The tensile strength variation with respect to curing temperature is calculated by Equation (2). The variability of the data and the presence of out layers which describes the statistics of various quartiles described by the numerical data are shown in Figure 8(b) also which reveals the maximum and minimum values of tensile strength and interquartile range.

Figure 9 describes the linear model summary which is used to diagnose the regression model.

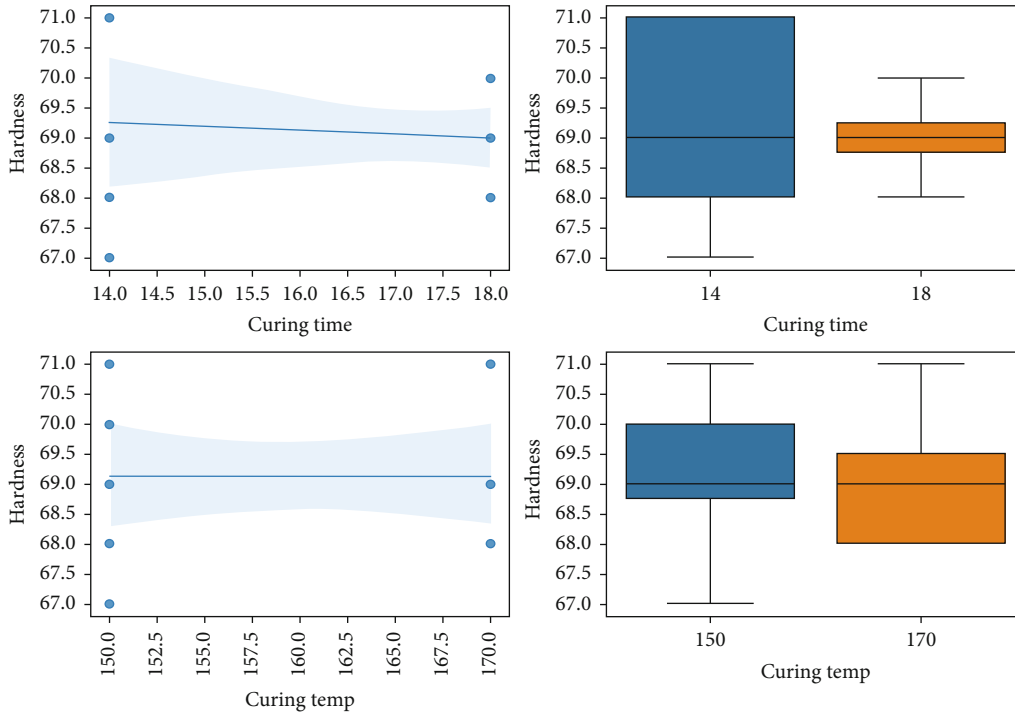


FIGURE 10: Hardness vs. curing time and hardness vs. curing temperature.

| Results: Ordinary least squares | | | | | | | Results: Ordinary least squares | | | | | | |
|---------------------------------|------------|--------|---------------------|---------|---------------------|------------|---------------------------------|---------------------|---------|---------|--------|---------|---------|
| Model: | OLS | | Adj. R-squared: | -0.095 | Model: | OLS | | Adj. R-squared: | -0.027 | | | | |
| Dependent variable: | Hardness | | AIC: | 38.8824 | Dependent variable: | Hardness | | AIC: | 38.1115 | | | | |
| Date: | 2023-02-22 | 16:26 | BIC: | 39.8523 | Date: | 2023-02-22 | 16:34 | BIC: | 39.0813 | | | | |
| No. observations: | 12 | | Log-likelihood: | -17.441 | No. observations: | 12 | | Log-likelihood: | -17.056 | | | | |
| Df model: | 1 | | F-statistic: | 0.04630 | Df model: | 1 | | F-statistic: | 0.7129 | | | | |
| Df residuals: | 10 | | Prob (F-statistic): | 0.834 | Df residuals: | 10 | | Prob (F-statistic): | 0.418 | | | | |
| R-squared: | 0.005 | | Scale: | 1.2857 | R-squared: | 0.067 | | Scale: | 1.2057 | | | | |
| Coef. | Std. err. | t | P > t | [0.025 | 0.975] | Coef. | Std. err. | t | P > t | [0.025 | 0.975] | | |
| Const | 67.7857 | 5.2664 | 12.8714 | 0.0000 | 56.0515 | 79.5199 | Const | 66.7000 | 2.6445 | 25.2226 | 0.0000 | 60.8078 | 72.5922 |
| Curing temp | 0.0071 | 0.0332 | 0.2152 | 0.8340 | -0.0668 | 0.0811 | Curing time | 0.1357 | 0.1607 | 0.8443 | 0.4182 | -0.2224 | 0.4939 |
| Omnibus: | 0.087 | | Durbin-Watson: | 2.176 | Omnibus: | 3.583 | | Durbin-Watson: | 1.714 | | | | |
| Prob (Omnibus): | 0.957 | | Jarque-Bera (JB): | 0.191 | Prob (Omnibus): | 0.167 | | Jarque-Bera (JB): | 1.280 | | | | |
| Skew: | 0.147 | | Prob (JB): | 0.909 | Skew: | 0.754 | | Prob (JB): | 0.527 | | | | |
| Kurtosis: | 2.457 | | Condition no.: | 2552 | Kurtosis: | 3.533 | | Condition no.: | 138 | | | | |

FIGURE 11: Linear model summary for hardness vs. curing time and hardness vs. curing temperature.

The independent parameter is chosen to be curing temperature (x), and the linear model is given in

$$\text{Tensile strength} = 4.4498 + 0.0199 \times \text{curing temperature.} \tag{4}$$

From the analysis, it is clear that, for every 1°C increase of curing temperature, the tensile strength will increase by 0.0199 N/mm².

3.5. Effect of Curing Time and Temperature on Hardness. Figure 10 shows the effect of curing time and curing temperatures on hardness which clearly shows the correlation

between the independent variables and dependent variables. The box plot shows the variability of data and the statistics of various quartiles. The maximum and minimum hardness values of the specimens are also described by the scatter and box plots. From Figure 10 and the linear model summary in Figure 11, it is clearly identified that the correlation between the hardness and independent variables such as curing temperature is very less compared with the variable curing time. This result indicates that there is very little influence on hardness of the fabricated vinyl polyester rubber due to curing temperature. The curing time makes an influence on hardness. But very small amount of hardness variation is recorded compared with tensile strength. The variation quantity is calculated by Equations (5) and (6).

The independent parameter is chosen to be curing time and curing temperature, and the linear model is given in

$$\text{Hardness} = 67.7857 + 0.0071 \times \text{curing temperature}, \quad (5)$$

$$\text{Hardness} = 66.7000 + 0.1357 \times \text{curing time}. \quad (6)$$

From the analysis, it is clear that, for every 1°C increase of curing temperature, the hardness value will increase by 0.0071HB N/mm², and 0.1357HB increases for every 1 sec curing time.

4. Conclusion

The development of poly vinyl rubber material for sealing applications has been successful, and the mechanical properties of the material have been investigated using various factors such as curing temperature, curing time, postcuring temperature, and postcuring time. The tensile strength and hardness of the material were analyzed using ASTM standard, and it was found that the specimen prepared at 150°C curing temperature, 18 min curing time, 50°C postcuring temperature, and 120 min postcuring time provides the highest tensile strength and better hardness value. A design of experiment (DOE) analysis was performed to determine the best values of the factors impacting the mechanical characteristics of the seal material. Simple regression analysis was used to find the influence of curing temperature and curing time on the tensile strength and hardness. The analysis showed that for every 1 second increase of curing time, the tensile strength will increase by 0.136 N/mm², and the hardness value will increase by 0.1357HB. Similarly, for every 1°C increase of curing temperature, the tensile strength will increase by 0.0199 N/mm², and the hardness value will increase by 0.0071HB. The study provides valuable information on the development and optimization of poly vinyl rubber material for sealing applications, and the results can be used to improve the mechanical properties of the material for better performance in sealing applications.

Data Availability

There is no data availability statement in this study.

Conflicts of Interest

The authors declare that they have no conflicts of interest.

References

- [1] W.-J. Lan, H.-X. Wang, X. Zhang, and S.-S. Chen, "Sealing properties and structure optimization of packer rubber under high pressure and high temperature," *Petroleum Science*, vol. 16, no. 3, pp. 632–644, 2019.
- [2] Y. Bai, Y. Yang, Z. Xiao, M. Zhang, and D. Wang, "Process optimization and mechanical property evolution of AlSiMg0.75 by selective laser melting," *Materials & Design*, vol. 140, pp. 257–266, 2018.
- [3] A. Dey and N. Yodo, "A systematic survey of FDM process parameter optimization and their influence on part characteristics," *Journal of Manufacturing and Materials Processing*, vol. 3, no. 3, p. 64, 2019.
- [4] E. Dhanumalayan and G. M. Joshi, "Performance properties and applications of polytetrafluoroethylene (PTFE)—a review," *Advanced Composites and Hybrid Materials*, vol. 1, no. 2, pp. 247–268, 2018.
- [5] D. Kai, N. Guanhua, X. Yuhang et al., "Effect of optimized pore structure on sealing performance of drilling sealing materials in coal mine," *Construction and Building Materials*, vol. 274, article 121765, 2021.
- [6] G. K. Gupta, P. K. Gupta, and M. K. Mondal, "Experimental process parameters optimization and in-depth product characterizations for teak sawdust pyrolysis," *Waste Management*, vol. 87, pp. 499–511, 2019.
- [7] W. Huang, G. Feng, H.-L. He, J.-Z. Chen, J.-Q. Wang, and Z. Zhao, "Development of an ultra-high-pressure rotary combined dynamic seal and experimental study on its sealing performance in deep energy mining conditions," *Petroleum Science*, vol. 19, no. 3, pp. 1305–1321, 2022.
- [8] G. Hu, P. Zhang, G. Wang, M. Zhang, and M. Li, "The influence of rubber material on sealing performance of packing element in compression packer," *Journal of Natural Gas Science and Engineering*, vol. 38, pp. 120–138, 2017.
- [9] P. Lu and R. J. K. Wood, "Tribological performance of surface texturing in mechanical applications—a review," *Surface Topography: Metrology and Properties*, vol. 8, no. 4, article 043001, 2020.
- [10] Y. Ding, R. Liu, J. Yao, Q. Zhang, and L. Wang, "Stellite alloy mixture hardfacing via laser cladding for control valve seat sealing surfaces," *Surface and Coatings Technology*, vol. 329, pp. 97–108, 2017.
- [11] K. Mohan, A. Seal, O. Krejcar, and A. Yazidi, "Facial expression recognition using local gravitational force descriptor-based deep convolution neural networks," *IEEE Transactions on Instrumentation and Measurement*, vol. 70, pp. 1–12, 2021.
- [12] D. A. D. Genuino, M. D. G. de Luna, and S. C. Capareda, "Improving the surface properties of municipal solid waste-derived pyrolysis biochar by chemical and thermal activation: optimization of process parameters and environmental application," *Waste Management*, vol. 72, pp. 255–264, 2018.
- [13] A. Karlekar, A. Seal, O. Krejcar, and C. Gonzalo-Martin, "Fuzzy k-means using non-linear *S-distance*," *Access*, vol. 7, pp. 55121–55131, 2019.
- [14] A. C. Bouali, E. A. Straumal, M. Serdechnova et al., "Layered double hydroxide based active corrosion protective sealing of plasma electrolytic oxidation/sol-gel composite coating on AA2024," *Applied Surface Science*, vol. 494, pp. 829–840, 2019.
- [15] Y. Bai, Y. Yang, D. Wang, and M. Zhang, "Influence mechanism of parameters process and mechanical properties evolution mechanism of maraging steel 300 by selective laser melting," *Materials Science and Engineering: A*, vol. 703, pp. 116–123, 2017.
- [16] A. M. Guerra, N. Mokni, P. Delage et al., "In-depth characterisation of a mixture composed of powder/pellets MX80 bentonite," *Applied Clay Science*, vol. 135, pp. 538–546, 2017.
- [17] H. A. Abdel-Aal, "Functional surfaces for tribological applications: inspiration and design," *Surface Topography: Metrology and Properties*, vol. 4, no. 4, article 043001, 2016.

- [18] C. L. Brown, D. E. Mulcahy, and R. A. Mittermaier, "Protein conformational dynamics measured by NMR relaxation," *Methods in Molecular Biology*, vol. 1688, pp. 227–258, 2018.
- [19] E. K. Oikonomou, G. Zachos, and P. Tsiakaras, "Hydrogen production via steam reforming of bio-ethanol: A review," *Renewable and Sustainable Energy Reviews*, vol. 100, pp. 286–305, 2019.
- [20] M. A. Hossain, K. H. Kim, J. H. Ahn, and J. J. Lee, "Recent advances in photocatalytic CO₂ reduction using metal-organic frameworks," *Journal of CO₂ Utilization*, vol. 39, article 101161, 2021.
- [21] K. Dong, G. Ni, B. Nie et al., "Effect of polyvinyl alcohol/aluminum microcapsule expansion agent on porosity and strength of cement-based drilling sealing material," *Energy*, vol. 224, article 119966, 2021.
- [22] H. Mahmood, F. Nart, and A. Pegoretti, "Effective recycling of end-of-life polyvinyl chloride foams in ethylene-propylene diene monomers rubber," *Journal of Vinyl and Additive Technology*, vol. 28, no. 3, pp. 494–501, 2022.
- [23] M. H. Alaaeddin, S. M. Sapuan, M. Y. M. Zuhri, E. S. Zainudin, and F. M. AL-Oqla, "Polyvinyl fluoride (PVF); its properties, applications, and manufacturing prospects," *IOP Conference Series: Materials Science and Engineering*, vol. 538, no. 1, article 012010, 2019.
- [24] S. Khouri, M. Behun, L. Knapcikova, M. S. AnnamariaBehunova, and A. Rosova, "Characterization of customized encapsulant polyvinyl butyral used in the solar industry and its impact on the environment," *Energies*, vol. 13, no. 20, p. 5391, 2020.
- [25] M. Kurakula and G. K. Rao, "Moving polyvinyl pyrrolidone electrospun nanofibers and bioprinted scaffolds toward multidisciplinary biomedical applications," *European Polymer Journal*, vol. 136, article 109919, 2020.
- [26] M. Q. Tanveer, A. Haleem, and M. Suhaib, "Effect of variable infill density on mechanical behaviour of 3-D printed PLA specimen: an experimental investigation," *SN Applied Sciences*, vol. 1, no. 12, p. 1701, 2019.
- [27] P. Jagadeesh, S. Mavinkere Rangappa, S. Siengchin et al., "Sustainable recycling technologies for thermoplastic polymers and their composites: a review of the state of the art," *Polymer Composites*, vol. 43, no. 9, pp. 5831–5862, 2022.
- [28] P. Jagadeesh, M. Puttegowda, S. M. Rangappa et al., "A comprehensive review on 3D printing advancements in polymer composites: technologies, materials, and applications," *The International Journal of Advanced Manufacturing Technology*, vol. 121, no. 1-2, pp. 127–169, 2022.
- [29] L. M. Júnior, L. M. de Oliveira, P. F. J. Bócoli, M. Cristianini, M. Padula, and C. A. R. Anjos, "Morphological, thermal and mechanical properties of polyamide and ethylene vinyl alcohol multilayer flexible packaging after high-pressure processing," *Journal of Food Engineering*, vol. 276, article 109913, 2020.
- [30] E. Kibirikštis, V. Mayik, R. Zatserkovna et al., "Study of physical and mechanical properties of partially biodegradable LDPE polymeric films and their application for printing and packaging," *Polymer Testing*, vol. 112, article 107646, 2022.